Field Test on Two Interior Insulation Systems with Large Thickness—Influence of Orientation and Airtightness

M. Stelzmann, Dipl.Ing. **B. Nusser, PhD** **U. Möller, PhD**

ABSTRACT

From the hygrothermal point of view, exterior insulation finishing systems (EIFS) are the preferred way to retrofit old buildings. However, in some cases EIFS are not possible to apply (e.g., for historic buildings, individual flats, or technical reasons). An interior insulation can be applied in such cases. Due to the dew-point shift and changed drying capacity of the wall, this might result in moisture and durability problems. There are different kinds of interior insulation systems and each one has its own way of moisture management. In this paper, the hygrothermal behavior of two different interior insulation systems with moderate vapor permeability and large insulation thickness will be discussed. A 200 mm EPS (expanded polystyrene) system and a 160 mm mineral wool system were monitored during a 18-month field test. Each system had been wall mounted on hollow block concrete masonry with orientation to South, West, and North. Temperature and relative humidity were monitored between interior insulation and the outer wall. The moisture content of the old plaster as well as the heat flux was measured. To test the impact of air leakage in the air barrier of the mineral wool system two elements with different numbers and sizes of leaks were investigated. Furthermore, hygrothermal simulations were verified with the collected data.

INTRODUCTION

From the building physics point of view, external insulation is preferred. However, in some cases external insulation is not possible either because of design, historic preservation, or technical or economic aspects. Interior insulation may be chosen in these cases. In contrast to a retrofitted wall with an exterior insulation, a subsequent interior insulation changes the building physics of an outer wall construction significantly. The dew-point zone moves inside the construction and increases the risk of condensation between the interior insulation and the original exterior wall (WTA 2009). Another cause for moisture entering in the construction is wind-driven rain. Because of reduced heat flux during winter months, the temperature in the outer wall decreases. Thus, the drying potential of the wall is reduced and the risk of freeze increased. For moderate vapor-permeable interior insulation systems, correctly dimensioned vapor barriers were used to guarantee airtightness and control the water vapor transport into the construction. The risk of condensation depends on the level of the quality of the airtightness of the inside insulation. In case of damaged airtightness, the humid warm air can flow into the interior insulation and condensate on the cold wall. The moisture performance of different inside insulation systems can be affected by the wind-driven rain and solar radiation in the different orientations. With the help of computer simulation of coupled heat and moisture transport (DIN 2007), building physic computations should be provided in any case while using interior insulation with large thickness. If the relative humidity turns under 95% in steady state, the evidence is provided (WTA 2014). This article describes the monitoring of a 200 mm EPS system (EPS) and a 160 mm mineral wool system (MW) under field conditions over a 18-month period. Further, the experimental set up, measurement results, and a comparison with hygrothermal simulations are presented. The research questions were: Did the moisture performance of the selected inside insulation systems work in large thickness, and is it possible to confirm the results in a simple and pragmatic simulation model?

M. Stelzmann is a doctoral student and **U. Möller** is a professor in the Institute of Building Construction, Structural Design and Building Physics, University of Applied Sciences, Leipzig, Germany. **B. Nusser** is the head of the building physic group at Holzforschung Austria, Vienna Austria (during project conduction he was employed at Saint-Gobain Isover, Ladenburg Germany).

EXPERIMENTAL SETUP

Construction of Test Walls

The test house is located in Ladenburg, Germany. The single-story building covered a ground floor area of 5.60 × 5.90 m. The exterior walls were built of hollow block concrete masonry, plastered on both sides with a thickness of 27.5 cm. The south, west, and north exterior test walls consist of six separate 65.5 cm (South and North) or 60.5 cm (West) wide wall sections. The individual wall sections were separated by a 6 cm gap. The sides and top of the wall sections were covered with a continuous air barrier. A bituminous sheeting was placed at the bottom side. The remaining gaps between the wall sections were filled with mineral wool. The wall sections were insulated with two different interior insulation systems. A picture of the test house and the ground plan with details are shown in Figure 1. Both interior insulation systems were installed on the south, west and north walls. Two additional wall sections were equipped with the mineral wool system on the north wall. Each of these two additional systems had one, respectively two, systematic holes in the smart vapor retarder and the drywall installation. The holes had a diameter of 5 mm. A system without air leak was used as reference. A historic wall construction with an heat transfer coefficient (U-factor) of 1.7 W/m^2·K was simulated with hollow block concrete masonry. The EPS system upgraded the U-factor of the construction to 0.15 W/m^2·K and the mineral wool system to 0.17 W/m^2·K (DIN 2008).

EPS System. The EPS system is based on expanded polystyrene bonded to a gypsum board. The insulation material has a thermal conductivity of 0.032 W/m·K. The diffusion equivalent air layer thickness (s_{di} value) of the EPS system was 11.1 m. The installation of the system had been carried out in a point bead method. Thereby the insulation board is fixed to the wall by a continuous mortar beat at the edge and mortar clump at the center of the boards back. For this field test, the interior insulation system had been installed with a insulation thickness of 200 mm. A sketch of the EPS system is shown in Figure 2.

Mineral Wool System. The mineral wool system is based on the insulating material mineral wool with a thermal conductivity of 0.032 W/m·K. A polyamide-based smart vapor retarder with variable vapor diffusion resistance reduces the entry of moisture from the room air. The variable s_{di} value of the mineral wool system was in the range between 0.5 and 25 m. An additional layer of a metal stud framing with drywall installation level protects the smart vapor retarder from damages. For this field test, the interior insulation had been installed with a mineral wool thickness of 160 mm. A sketch of the mineral wool system is shown in Figure 3.

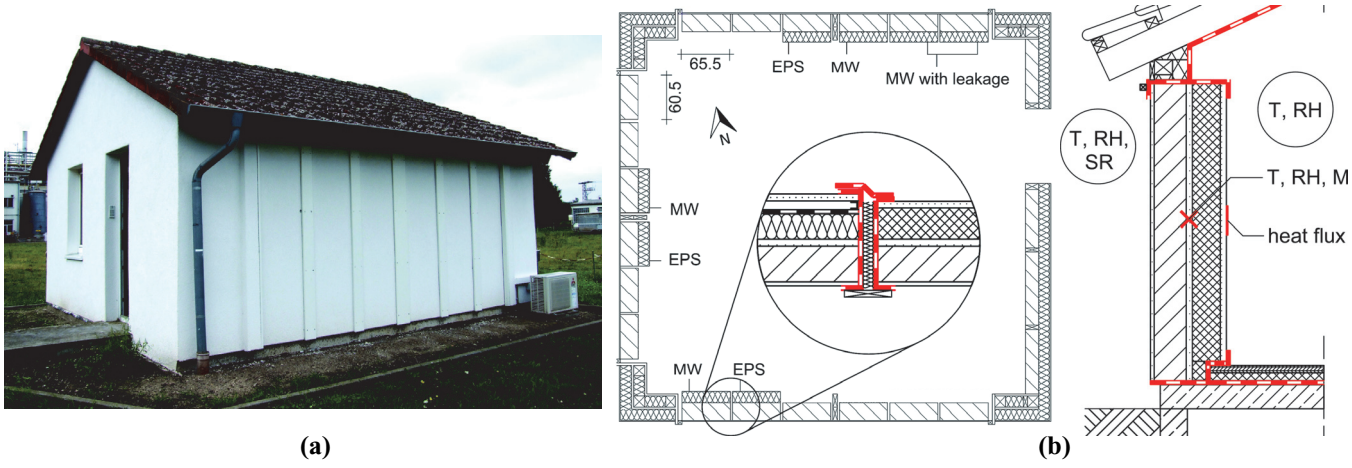

Figure 1 *(a) A picture of the test house in Ladenburg and (b) ground plan and sectional view with wall sections, marked positions of sensors (see Monitoring System section), and sealing layer.*

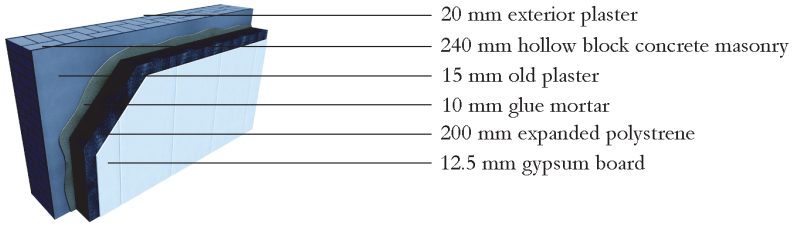

Figure 2 *Sketch of the EPS system with material legend (Bäumler 2013).*

Wind-Driven Rain Resistance

Referring to DIN (2014), the building was located in Stress Zone 2 with medium loads of wind-driven rain (WDR). Possible influences of moisture from WDR were therefore excluded by measuring the water absorption coefficient (W_w value) of the external plaster system. According to the German standard (DIN 2014) and technical bulletin (WTA 2009), a W_w value of the external plaster with 0.5 kg/(m$^2\cdot\sqrt{h}$) should not be exceeded. The water absorption coefficient was measured by the help of a nondestructive *in situ* technology presented in Möller and Stelzmann (2013) and Stelzmann et al. (2015). The measured W_w value of the external plaster system was 0.3 kg/(m$^2\cdot\sqrt{h}$). Thus, with a low W_w value of the external plaster in consideration with a single-story test building and an existing overhang of the roof, effects of WDR could be neglected in this study.

Monitoring System

To study the heat transmission resistances, heat flux plates (Q; sensor type Almemo FQA019C) were attached to the inner surface of the interior insulation at walls on the south, west and north side (see Figure 4). For the investigation of the insulation systems, a combined sensor for temperature (T) and relative humidity (RH; sensor type Almemo FHAD46-2), as well as a sensor for determining the moisture content (M; sensor type Brookhuis FME moisture meter) of the old plaster, were installed at the top, center, and bottom of the wall sections. In this paper, only the center position was discussed. The measurement of the relative humidity was carried out through a capacitive measuring principle. To make limited statements of moisture content of the old plaster, the electrical-conductivity based FME sensor was used. However, in laboratory tests, the FME with the calibration curve plaster was able to differentiate between the capillary and sorption moisture water region of plaster material. Thereby, the FME was able to assess the moisture content in case of relative humidity of over 95% rh. As seen in Figure 4, the sensor wiring was guided out laterally inside the old interior plaster from the wall sections. Thus, the insulation layer was not penetrated. Diffuse and direct solar radiation (SR) was determined using a sensor type Almemo FLA613GS-SDEK. With the exception of moisture content, the Almemo 5690-1 was used for automatically recording data. The moisture content was recorded by manual reading once a week. By an air-conditioning system (heating and cooling) combined with a relative-humidity-controlled humidifier (type Seliger Fogstar 300), the indoor climate was adjusted to standard climate in accordance to (DIN 2007).

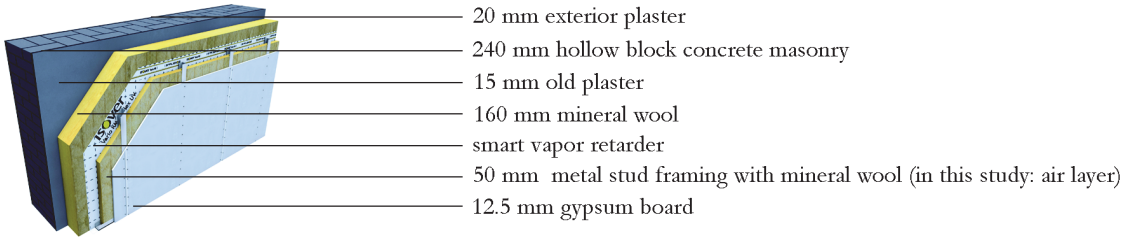

Figure 3 *Sketch of the mineral wool system with material legend (Bäumler 2013). The cavity between the metal stud framing was not insulated in these investigations.*

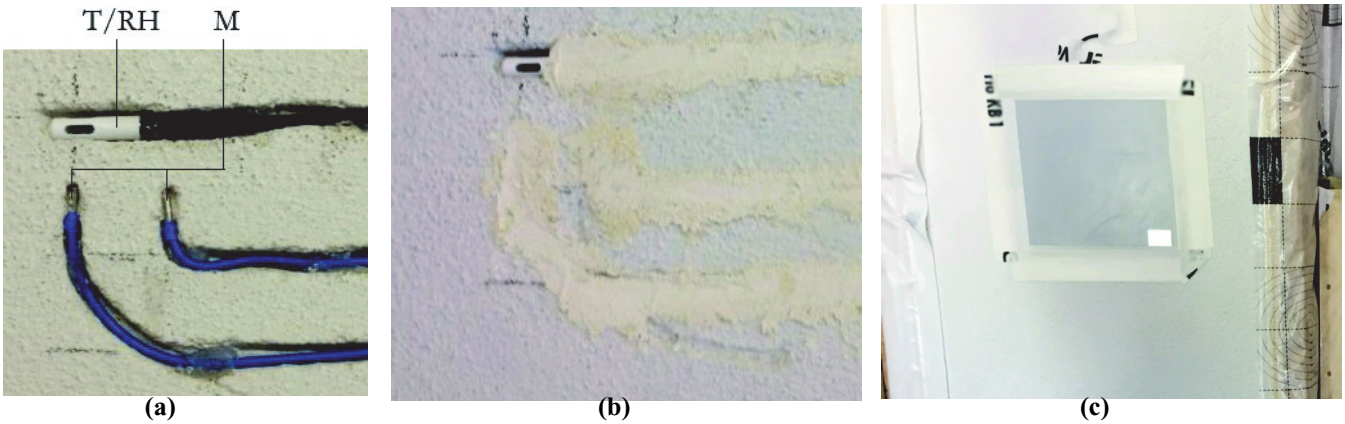

Figure 4 *(a) Embedded sensors in plaster, (b) cable slots were filled with plaster, and (c) selected heat flux plate.*

EXPERIMENTAL RESULTS

In the following section, a few results from the field test are presented (Stelzmann and Möller 2015). The climatic conditions inside and outside as well as the moisture behavior between the old plaster and insulation are shown. The results consider a 18-month period from October 1, 2014 to April 1, 2016. The installation of the surveyed interior insulation systems took place on October 17, 2014.

Conditions

The measurement data of the indoor and outdoor conditions are shown in Figure 5. The outdoor climate in 2014/2015 showed a typical trend for the location Ladenburg, Germany. The average outdoor temperature was 12°C with an average relative humidity of 78 %. The room temperature varied between 20°C and 25°C. Inside the test house, the relative humidity followed a sinusoidal course of a normal occupation in accordance to DIN (2007). The air-conditioning system was deactivated from October 1, 2014 to November 27, 2014. The results of relative humidity tests in test wall sections did not show a significant drying or wetting in this time. However, the inside climate nearly followed the standard climate in accordance to DIN (2007).

Thermal Performance

The heat transfer coefficients (U-factor) of the studied wall sections were determined by measuring the heat flux density from January 20, 2015 to January 28, 2015. Only data between 18:00 and 5:50 with a temperature difference of ≥20 K between inside and outside were considered. For calculating the U-factor in W/(m^2·K), the mean of measured heat flux in W/m^2 was divided by the mean of temperature difference between inside and outside in K. These measured results are compared to the theoretical calculated U-factor in Figure 6. The U-factor of the original wall was not tested in field. The theoretical transmission heat loss has been reduced by more than 90 % using interior insulation. The calculated U-factors were higher due to production-related material differences.

Moisture Performance

The moisture performance of interior insulation was assessed by the presence of liquid water on the old plaster. Usually this is the case at a relative humidity higher than 95%. The direction that moisture vapor flowed in inside the insulation is mainly from room humidity into the condensation zone at the old plaster in winter and from there to the inner and outer wall surfaces in summer. The results of the relative humidity and moisture content of the plaster at EPS system and mineral wool system are shown in Figure 7.

The EPS system shows an increased relative humidity of over 95% on the western and northern building sides from January to June in 2015. The moisture content of the plaster remains at a low level of under 1 M% over the entire study period. The installation moisture from the glue of the EPS system was responsible for the higher relative humidity in the first year. In March 2016 the 95% rh level was exceeded. It remains to be seen whether the relative humidity stays permanently below 95% for the remainder of 2016. The relative humidity of the mineral wool system remained below 95% over the entire period of investigation (see Figure 8). The lowest values were detected at the southern wall. The moisture content of the plaster also remained at a low level of under 1 M %. In contrast to the EPS system, there was no additional installation moisture brought into the construction.

Effects of Orientation

For testing effects of different orientations to the hygrothermal behavior, the two studied interior insulation systems were installed on the south, west and north wall (see Figures 7 and 8). As a result, the relative humidity tended to show lower values in the South and higher values in the North. The values of the western side tended to vary in between. Differences in relative humidity were attributable to temperature influence. By higher temperatures in the wall, moisture was driven inwards. Differences of measurement results in moisture content were rather small. The effect was largely solar radiation based.

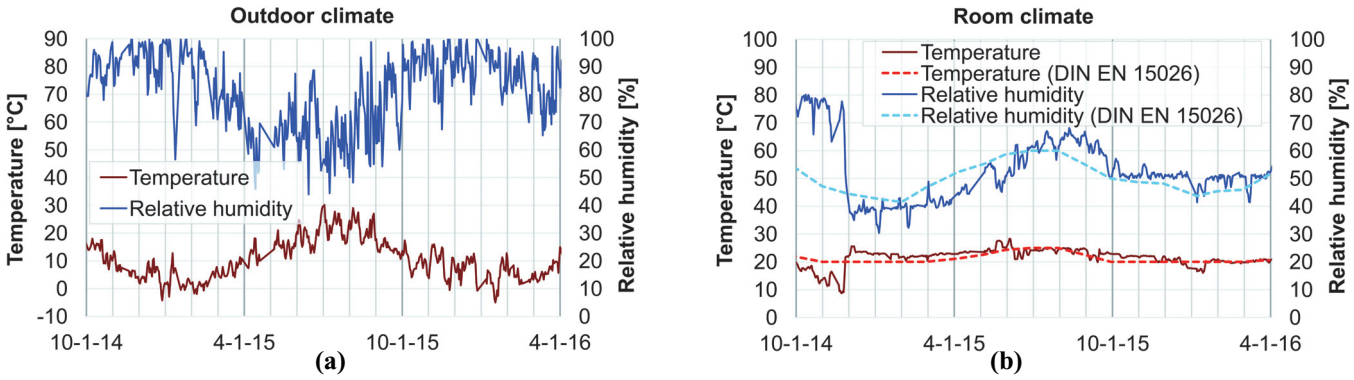

Figure 5 *(a) Outdoor and (b) room climate.*

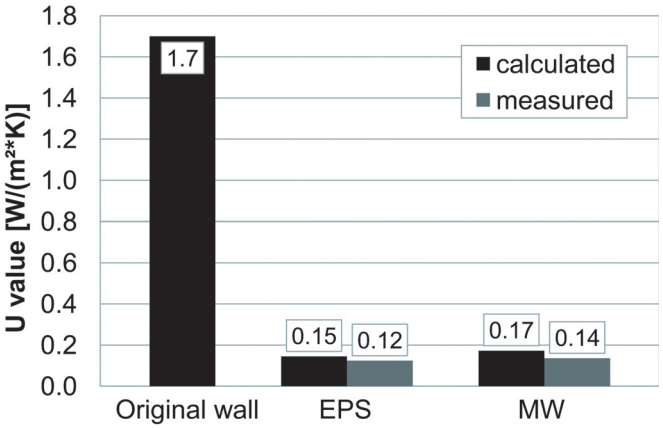

Figure 6 *Comparison of calculated and measured heat transfer coefficients.*

Effects of Leakage in Airtightness of Mineral Wool System

Two wall sections of the mineral wool system were modified by 5 mm holes in the smart vapor retarder and inner lining. Figure 9(a) shows a sketch for testing leakage in the airtightness layer of the insulation system. The airtightness of the wall is already guaranteed by interior and exterior plaster. A fan moved the air in the room. Differences in relative humidity might justified by an airflow from the room to condensation zone. In contrast to Fox et al. (2014), in this study no air pump was used to inject an airflow inside the insulation. An airflow could drive temperature-based convection between top and bottom hole (two leaks). Figure 9(b) gives the conditions in the mineral wool system with holes and thermal-stack-based air pressure difference (P) between the holes in two leaks test. The examined variants behaved similarly. The system with no leakage showed mostly higher relative humidities than the other two systems with leaks. In the used test setup, an effect

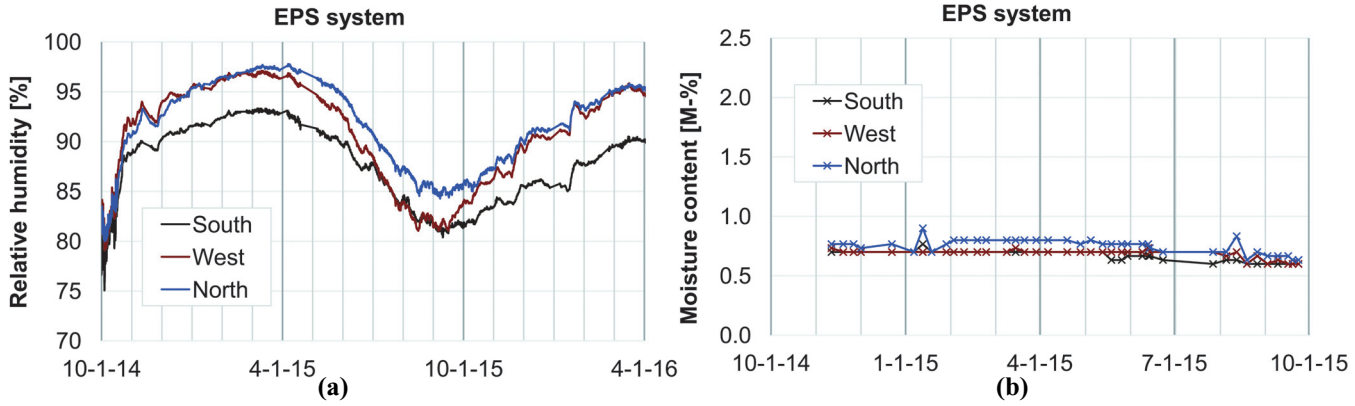

Figure 7 *Comparison of (a) relative humidity and (b) moisture behavior of the EPS system for the orientations South, West, and North.*

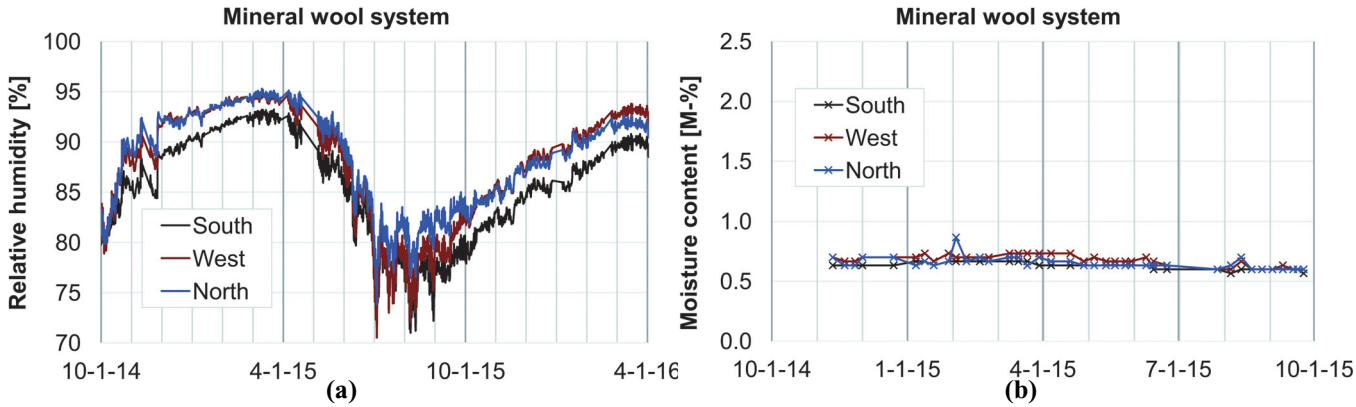

Figure 8 *Comparison of (a) relative humidity and (b) moisture behavior of mineral wool system for the orientations South, West, and North.*

of the holes in the smart vapor retarder and inner lining could not be found. The measured temperature difference between the top and bottom hole was about 1 K in winter. From these data the pressure difference (P) was approximated by Equation 2.14 in Hens (2012). In this study, air pressure differences by thermal stack were small (two holes). The airtight exterior plaster prevented an airflow between inside and outside and the diameter and numbers of holes were rather small. The airflow resistance of the mineral wool could explain the results too. As a result, the collected data showed an existing hygrothermal robustness of the studied mineral wool system.

LONG-TERM TRENDS WITH HYGROTHERMAL SIMULATION

If the relative humidity at the condensation zone turns under 95% in the long term, the inside insulation system is proved (WTA 2014). Long-term simulation can indicate wetting or drying trends. To conduct the hygrothermal simulation (DIN 2007) the program Delphin 5.8 (Nicolai et al. 2010) was used in one-dimensional mode. Measured data of indoor and outdoor climate (temperature and relative humidity) as well as material data of the tested inside insulation systems was available. For material data of the hollow block concrete masonry the Delphin database (Scheffler and Plagge 2009) was used. For the simulation model of mineral wool system, a vapor retarder with fixed vapor permeability was used (s_{di} = 2.5 m). The influence of wind-driven rain (WDR) was not included in the simulations. For the consideration of initial conditions or the installation moisture, experience-based assumptions were made (DIN 2010). Due to lack of exact input data (e.g., initial conditions, material data) the simulations could only provide limited statements. However, with the conducted simulation, trends could be stated. The simulation results of the two studied interior insulation systems for five years are shown in Figure 10. Additionally, the measurement data was overlaid onto the graphs. Simulation and measurement of the mineral wool system demonstrated a similar trend. The EPS system revealed a poor correlation of simulation and measurement results. There were doubts as to whether the simulation results of EPS

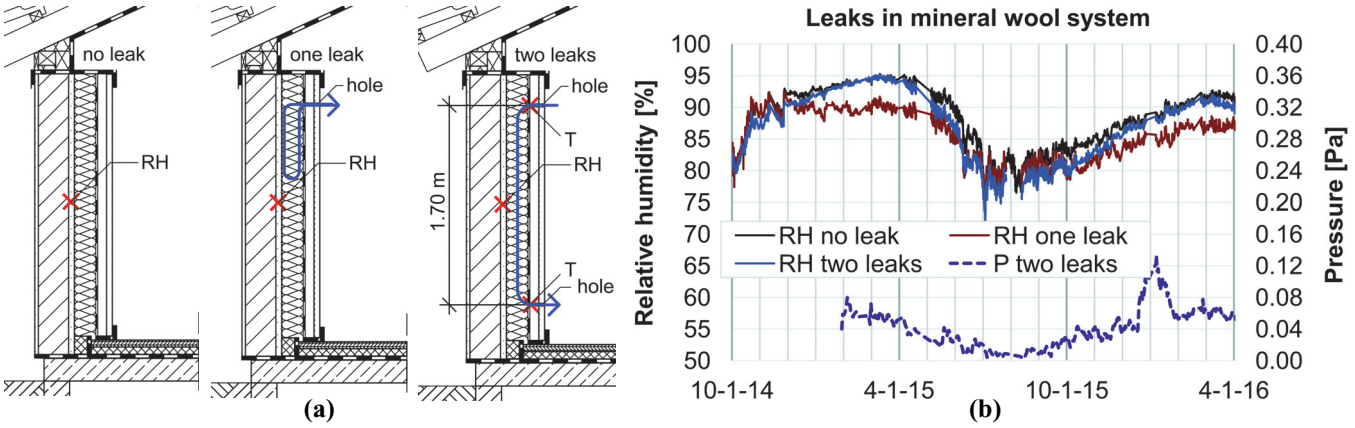

Figure 9 *(a) A sketch of test setup with leaks and (b) behavior of relative humidity for inner plaster of mineral wool system with and without leaks and vertical air pressure difference between top and bottom hole.*

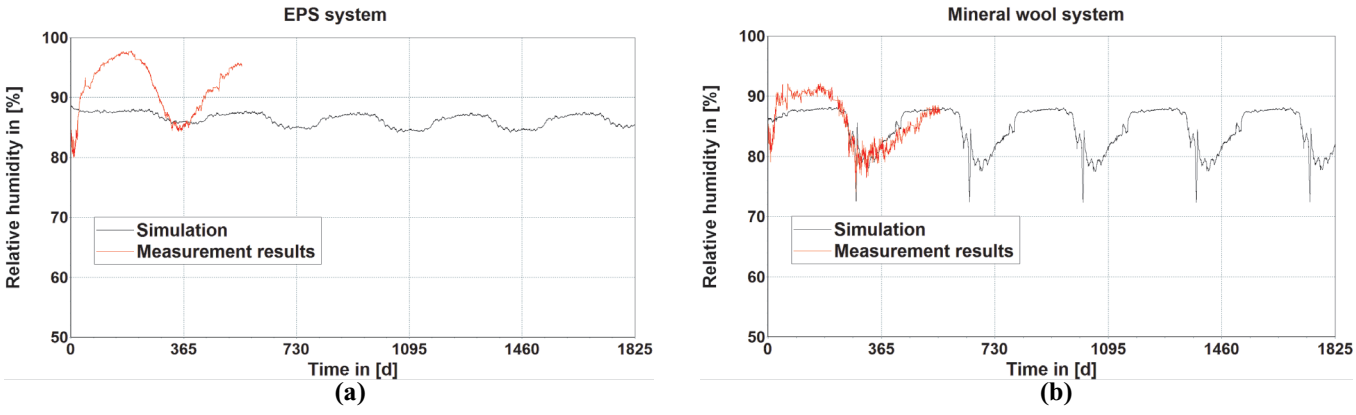

Figure 10 *Comparison of simulation and measurement results for relative humidity of (a) EPS and (b) MW.*

system could predict the moisture behavior. Deviations at the beginning were caused by the installation duration. Assumptions of material data can be responsible for differences in moisture behavior. The simulation results indicated a trend towards lower relative humidities. Already, starting from the second simulated year, both interior insulation systems reached a steady state. As a result, the created simple hygrothermal simulation did not match with the recorded data. The explanation for this could be the fact that material data was used from database, simulation was designed in one-dimensional mode, and no WDR data was included.

CONCLUSIONS

An EPS and a mineral-wool-based interior insulation system with large insulation thicknesses were monitored in a test house for an 18-month period. In the study, exterior walls without thermal bridges were tested. The test setup was realized with a high wind-driven rain resistance; thus, entering moisture by wind-driven rain was significantly limited. Still, outdoor relative humidity, surface condensation, and inward vapor flow could have some wetting impact on the moisture of the masonry. The results demonstrated a theoretical reduction of transmission heat loss by the interior insulation systems of more than 90%. The EPS system showed relative humidity above 95 % in the condensation zone in both years. The relative humidity of the mineral wool system remained below 95% over the entire period of investigation. Moisture effects by different orientations in both systems were detected. The south wall showed the lowest and the north walls the highest relative humidities. This effect was solar radiation based. Furthermore, effects of leaks in the inner airtight layers of the mineral wool system were investigated. In the specific experimental design with an airtight exterior plaster, no significant hygrothermal differences between the airtight and leaky systems were found. Results of a simple hygrothermal simulation study did not confirm with the measured data. To improve the simulation, some more climate and material data should be implemented. The collected and analyzed data showed that the highly insulated interior systems retrofit strategies are possible.

REFERENCES

Bäumler, S. 2013. Aktuelle Untersuchungen der SAINT-GOBAIN Innendämm-Systeme. wksb – Zeitschrift für Wärmeschutz Kälteschutz Schallschutz Brandschutz 69:43–48.

DIN. 2007. DIN EN 15026, *Hygrothermal performance of building components and building elements—Assessment of moisture transfer by numerical simulation*. Berlin: Deutsches Institut für Normung e.V.

DIN. 2008. DIN EN ISO 6946, *Building components and building elements—Thermal resistance and thermal transmittance—Calculation method*. Berlin: Deutsches Institut für Normung e.V.

DIN. 2010. DIN EN ISO 10456, *Building materials and products—Hygrothermal properties—Tabulated design values and procedures for determining declared and design thermal values*. Berlin: Deutsches Institut für Normung e.V.

DIN. 2013. DIN 4108-2, *Thermal protection and energy economy in buildings—Part 2: Minimum requirements to thermal insulation*. Berlin: Deutsches Institut für Normung e.V.

DIN. 2014. DIN 4108-3, *Thermal protection and energy economy in buildings—Part 3: Protection against moisture subject to climate conditions—Requirements and directions for design and construction*. Berlin: Deutsches Institut für Normung e.V.

Fox, M., J. Straube, H. Ge, and T. Trainor. 2014. Field test of hygrothermal performance of highly insulated wall assemblies. In 14th Canadian Conference on Building Science and Technology, Toronto. October 28–30.

Hens, H. 2012. *Building physics—Heat, air and moisture: Fundamentals and engineering methods with examples and exercises*, 2nd edition. Berlin: Ernst & Sohn. ISBN 978-3-433-03027-1, 134–35.

Möller, U., and M. Stelzmann. 2013. In-Situ-Messgerät für die zerstörungsfreie Messung der Wasseraufnahme. in: 2. Internationaler Innendämmkongress vom 12. bis 13. April 2013 in Dresden, Tagungsunterlagen, Grunewald, J., Plagge, R. (Hrsg.), Dresden: TU-Dresden, Institut für Bauklimatik, 188–97.

Nicolai, A., J. Grunewald, R. Plagge, and G. Scheffler. 2010. Development of a combined heat, moisture, and salt transport model for unsaturated porous building materials. In Simulation of Time Dependent Degradation of Porous Materials, Research Report on Priority Program DFG SPP 1122, eds. L. Franke, G Deckelmann, and R. Espinosa-Marzal, Cuilliver Verlag. ISBN 978-3-86727-902-4. 67–84.

Scheffler, G. and R. Plagge. 2009. A whole range hygric material model: Modeling liquid and vapour transport properties in porous media. *Int. J. Heat Mass Transfer*, doi:10.1016/j.ijheatmasstransfer. 2009.09.030.

Stelzmann, M., U. Möller, and R. Plagge. 2015. Water-absorption-measurement instrument for masonry façades, in: ETNDT6, *Emerging Technologies in Non-Destructive Testing* 6, 27–29 May 2015, Brussels, Belgium.

Stelzmann, M., and U. Möller. 2015. Saint-Gobain Innendämmsysteme im Freilandversuch–Abschlussbericht.

WTA. 2009. WTA Guideline 6-4, Inside insulation according to WTA I: Plenary guide. Stuttgart: Wissenschaftlich-Technische Arbeitsgemeinschaft für Bauwerkserhaltung und Demkmalpflege e.V.

WTA. 2014. WTA Guideline 6-5, *Interior insulation according to WTA II: Evaluation of internal insulation systems with numerical design methods*. Stuttgart: Wissenschaftlich-Technische Arbeitsgemeinschaft für Bauwerkserhaltung und Demkmalpflege e.V.